



Low core loss of Fe₈₅Si₂B₈P₄Cu₁ nanocrystalline alloys with high B_s and B₈₀₀

Takeshi Kubota^{a,*}, Akihiro Makino^a, Akihisa Inoue^b

^a Institute for Materials Research, Tohoku University, 2-1-1 Katahira, Aoba-ku Sendai 980-8577, Japan

^b Tohoku University, 2-1-1 Katahira, Aoba-ku Sendai 980-8577, Japan

ARTICLE INFO

Article history:

Received 6 July 2010

Received in revised form

30 September 2010

Accepted 2 November 2010

Available online 10 November 2010

Keywords:

Low core loss

High magnetic flux density

Nanocrystalline soft magnetic alloy

Hetero-amorphous alloy

ABSTRACT

The Fe–Si–B–P–Cu nanocrystalline alloys exhibit high saturation magnetic flux density (B_s) as well as good soft magnetic properties such as low coercivity, high effective permeability and low magnetostriction after nanocrystallization. In this paper, the Fe₈₅Si₂B₈P₄Cu₁ alloy has been newly developed. On the viewpoint of magnetic softness, the Fe₈₅Si₂B₈P₄Cu₁ nanocrystalline alloy reveals low core loss (W) at a commercially frequency of 50 Hz in the maximum induction (B_m) range of up to 1.75 T, and the W in the B_m range of less than 1.8 T is smaller than that of the highest-graded oriented Si-steel due to high magnetic flux density at 800 A/m (B_{800}) of above 1.8 T and excellent magnetic softness originated from much higher Fe content and uniform nanocrystalline structure with small magnetostriction. The electrical resistivity (ρ) is relative higher than Si-steels. Thus the Fe–Si–B–P–Cu alloys are attractive for applying to magnetic parts such as motors, transducers, choke-coils and so-forth.

© 2010 Elsevier B.V. All rights reserved.

1. Introduction

Si-steel [1] having rather high saturation magnetic flux density (B_s) of about 2 T, good productivity and low material cost is still now the most major soft magnetic material in practical use for many kinds of transformers and motors. However, considering recent energy problem, it is required that development of the new soft magnetic material with high B_s almost comparable to the Si-steels combined with excellent magnetic softness for decreasing electrical consumption in many kind of apparatus, minimizing the physical dimensions of components and reducing the weight for the vehicle installation. The conventional nanocrystalline soft magnetic alloys [2,3] such as Fe–Si–B–M–Cu and Fe–M–B (M: non-magnetic early transition metals), and their derivatives exhibit excellent magnetic softness and relative high B_s of 1.2–1.7 T. However the alloys inevitably include a large amount of M elements such as Nb, Zr, Mo, etc. to realize the nanocrystallized structure [4–6], and addition of the M elements results in a remarkable decrease of B_s which is inferior to around 2 T of Si steel and significantly larger materials costs. Fe–Co–Hf–B–Cu alloy exhibits higher B_s of about 1.8 T [7], however magnetic softness is much inferior to the above mentioned nanocrystalline alloys.

Recently, it has been reported that the simultaneous addition of P and Cu affects refinement of α -Fe phase precipitated in the as-quenched Fe–Nb–B [8] and Fe–Si–B [9,10] alloys with high Fe

content exceeding the limit for the formation of a single amorphous phase. Furthermore, these alloys can form uniform nanocrystalline structure after annealing [11,12]. Fig. 1 shows the outer appearance of the melt-spun Fe_{84.3}Si₄B₈P₃Cu_{0.7} alloy ribbon with 6 mm in width. All the melt-spun Fe–Si–B–P–Cu alloys were easily produced in air atmosphere and found to be completely ductile. Fig. 2 shows the transmission electron microscopy images of the melt-spun Fe_{83.3}Si₄B₈P₄Cu_{0.7} alloy in the as-quenched and crystallized states [11]. The as-quenched alloy can form a hetero-amorphous structure composed of a large number of α -Fe crystals with less than 3 nm in diameter and an amorphous matrix by the simultaneous addition of 4 at%P and 0.7 at%Cu to Fe₈₄Si₄B₁₂ alloy, and the heterogeneity in the as-quenched state possibly acts as the nucleation site for the nanocrystallization of α -Fe phase. These Fe_{83.3–84.3}Si₄B₈P_{3–4}Cu_{0.7} nanocrystallized alloys exhibit rather high B_s of above 1.8 T and excellent magnetic softness due to high Fe content and homogeneous nanocrystalline structure with a small magnetostriction. In this paper, we investigate the magnetic and electric property of the melt-spun Fe₈₅Si₂B₈P₄Cu₁ alloy.

2. Experimental

Fe₈₅Si₂B₈P₄Cu₁ alloy ingot was prepared by an arc melting with mixtures of Fe (99.98 mass%), Si (99.998 mass%), B (99.5 mass%), Cu (99.99 mass%) and pre-melted Fe₃P (99.9 mass%) in a high-purified Argon atmosphere. A single-roller melt-spinning method in air atmosphere was used to produce the rapidly solidified ribbons with about 6 mm in width and 18–20 μ m in thickness. The alloy compositions are nominally expressed since the difference between nominal and chemical analyzed composition was negligibly small, and expressed in atomic percentage. For the Fe₇₈Si₉B₁₃ typical amorphous alloy and oriented/non-oriented Si-steels, commercialized materials were used. Crystallization temperature of melt-spun alloys was evaluated with a differential scanning calorimeter (DSC) at a heating rate

* Corresponding author at: Tel.: +81 22 215 2158; fax: +81 22 215 2137.
E-mail address: kubott@imr.tohoku.ac.jp (T. Kubota).

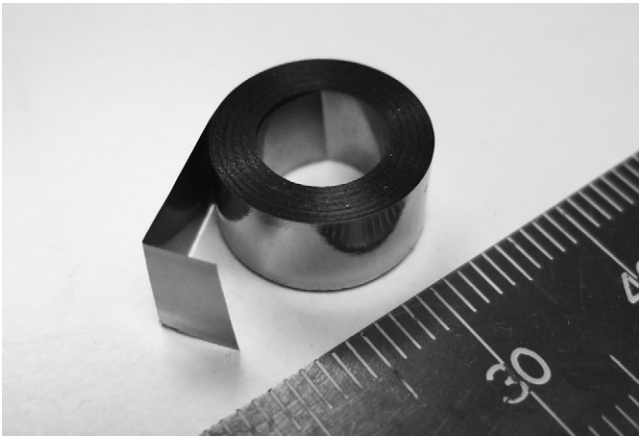


Fig. 1. Outer appearance of the melt-spun $\text{Fe}_{84.3}\text{Si}_4\text{B}_8\text{P}_3\text{Cu}_{0.7}$ alloy ribbon with 6 mm in width and complete ductility.

of 0.67°C/s under an Argon flow. The structures in as-quenched and annealed states were identified by X-ray diffractometry (XRD) and transmission electron microscopy (TEM), and the average grain size was estimated by TEM observations. Heat treatment for the crystallization was carried out for 600 seconds (s) in a vacuum atmosphere under the non-magnetic field. The annealing temperatures were decided to referring the crystallization temperature obtained from the result of DSC

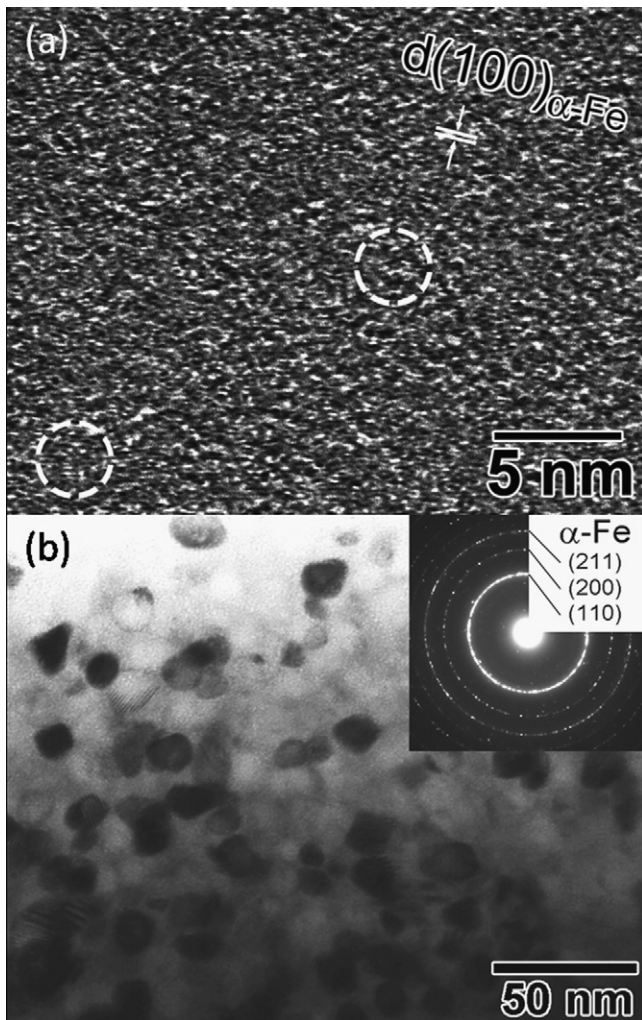


Fig. 2. High resolution TEM image of as-melt-spun $\text{Fe}_{83.3}\text{Si}_4\text{B}_8\text{P}_4\text{Cu}_{0.7}$ alloy (a), and bright field image and selected area electron diffraction pattern of the alloy annealed at 475°C for 600 s [11].

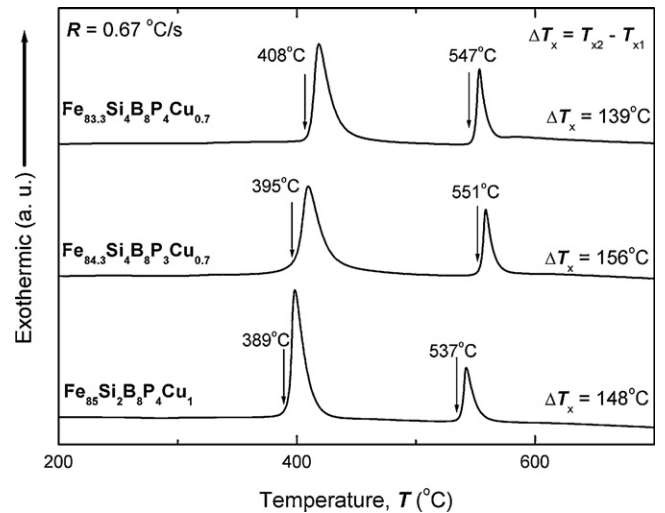


Fig. 3. DSC traces for the melt-spun $\text{Fe}_{83.3}\text{Si}_4\text{B}_8\text{P}_4\text{Cu}_{0.7}$, $\text{Fe}_{84.3}\text{Si}_4\text{B}_8\text{P}_3\text{Cu}_{0.7}$ and $\text{Fe}_{85}\text{Si}_2\text{B}_8\text{P}_4\text{Cu}_1$ alloys.

trace. $\text{Fe}_{78}\text{Si}_9\text{B}_{13}$ amorphous alloy was annealed at 380°C for 7.2 ks, and Si-steels were used as received. Saturation magnetic flux density (B_s) and coercivity (H_c) were measured by a vibrating sample magnetometer (VSM) and a DC B-H loop tracer under maximum applied fields of 800 kA/m and 800 A/m, respectively. Magnetic flux density at 800 A/m (B_{800}) was also measured by a DC B-H loop tracer. Effective permeability (μ_e) at 1 kHz and core loss (W) at 50 Hz were measured by a vector impedance analyzer under a field of 0.4 A/m and an AC B-H analyzer operated under sinusoidal input voltage, respectively. Saturation magnetostriction (λ_s) was measured in an applied field of up to 800 kA/m by the strain gauge method. Electrical resistivity (ρ) was measured by a four-terminal method. Density was measured by the Archimedeian method with n-tridecane. All of the characteristics were measured for a single sheet shape.

3. Results and discussion

The XRD profile of the melt-spun $\text{Fe}_{85}\text{Si}_2\text{B}_8\text{P}_4\text{Cu}_1$ alloy showed no distinct diffraction peaks implying any crystalline phases, it is thought that the melt-spun alloy also formed a hetero-amorphous structure as well as the $\text{Fe}_{83.3}\text{Si}_4\text{B}_8\text{P}_4\text{Cu}_{0.7}$ alloy [10]. Fig. 3 shows the DSC traces for melt-spun $\text{Fe}_{83.3}\text{Si}_4\text{B}_8\text{P}_4\text{Cu}_{0.7}$, $\text{Fe}_{84.3}\text{Si}_4\text{B}_8\text{P}_3\text{Cu}_{0.7}$ and $\text{Fe}_{85}\text{Si}_2\text{B}_8\text{P}_4\text{Cu}_1$ alloys. All the alloys crystallize through two exothermic peaks. The first and the second exothermic peaks were confirmed to be caused by the structural changes from “hetero-amorphous” to “ α -Fe + residual amorphous matrix” and finally to “ α -Fe + some compound phases”. The ΔT_x of the alloys were above 130°C , which are wider than 81°C of $\text{Fe}_{84}\text{Si}_4\text{B}_{12}$, 94°C of $\text{Fe}_{83.3}\text{Si}_4\text{B}_{12}\text{Cu}_{0.7}$ and 104°C of $\text{Fe}_{84}\text{Si}_4\text{B}_8\text{P}_4$ [12]. It should be noted that wider ΔT_x easily forms the “ α -Fe + residual amorphous” structure without any compound phases by annealing in the temperature range between T_{x1} and T_{x2} .

Fig. 4 shows the annealing temperature dependence of B_{800} and B_s for the melt-spun $\text{Fe}_{85}\text{Si}_2\text{B}_8\text{P}_4\text{Cu}_1$ alloy. The as-quenched alloy exhibited 1.14 T of B_{800} and 1.58 T of B_s . On the other hands, drastic change in B_{800} was found after annealing in the temperature range of above 300°C . This enhancement of B_{800} must be originated from following two reasons. The structure annealed at 300°C sustained almost the same as as-quenched structure confirmed by a TEM observation. Therefore B_s showed little change. However B_{800} was close to B_s , magnetic softness was enhanced due to relaxation the stress induced during melt-spinning. On the other hands, B_s gradually increased with further increase in annealing temperature. Although the onset crystallization temperature of α -Fe is 389°C estimated by the DSC trace, the heat treatment was carried out for 600 s in this study. Therefore crystallization gradually and partially occurred in the range of from about 330°C . On the curve of the B_{800} , the value gradually increased up to 1.82 T

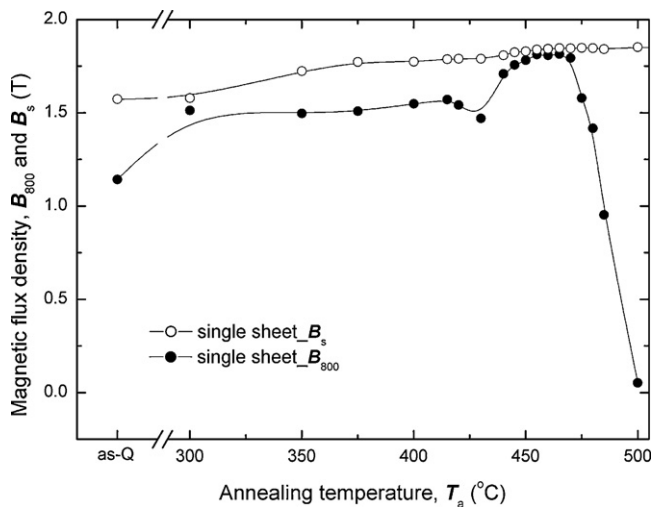


Fig. 4. Annealing temperature dependence of B_{800} and B_s for the melt-spun $\text{Fe}_{85}\text{Si}_2\text{B}_8\text{P}_4\text{Cu}_1$ alloy.

with increasing annealing temperature and suddenly decreased at 475 °C. In contrast, B_s values monotonically increased with increasing annealing temperature and reached to 1.846 T at 500 °C and to a maximum of 1.852 T at 500 °C. The B_{800} of above 1.8 T in the alloy annealed in the temperature range of 450–470 °C implies that the crystallized alloy exhibit good magnetic softness due to nanocrystallization by appropriate annealing. Based on the result of the annealing temperature dependence of H_c , the H_c curve also indicated same tendency. The alloy annealed in the temperature range of 445–465 °C exhibits low H_c value less than 10 A/m (not shown here) and annealed structure is composed of nano sized α -Fe and amorphous phases confirmed by XRD. Fig. 5 shows the annealing temperature dependence of ρ for the melt-spun $\text{Fe}_{85}\text{Si}_2\text{B}_8\text{P}_4\text{Cu}_1$ alloy. Here the data of the $\text{Fe}_{85}\text{Si}_2\text{B}_8\text{P}_4\text{Cu}_1$ alloy are also shown for comparison. The as-quenched $\text{Fe}_{85}\text{Si}_2\text{B}_8\text{P}_4\text{Cu}_1$ alloy exhibited ρ of 1.27 $\mu\Omega\cdot\text{m}$. This value is slightly lower than 1.33 $\mu\Omega\cdot\text{m}$ for the as-quenched $\text{Fe}_{83.3}\text{Si}_4\text{B}_8\text{P}_4\text{Cu}_{0.7}$ alloy and 1.35 $\mu\Omega\cdot\text{m}$ for the $\text{Fe}_{78}\text{Si}_9\text{B}_{13}$ amorphous alloy. In annealed states, the ρ suddenly decreased at around 350 °C and reached to about 0.80 $\mu\Omega\cdot\text{m}$. In the annealing temperature range of from 400 to 450 °C, the ρ gradually decreased and reached to 0.74 $\mu\Omega\cdot\text{m}$ at 450 °C. By further increase in annealing temperature the alloy kept decreasing trend and finally reached to about 0.6 $\mu\Omega\cdot\text{m}$ at 500 °C. Here comparing with the result of $\text{Fe}_{83.3}\text{Si}_4\text{B}_8\text{P}_4\text{Cu}_{0.7}$ alloy, the increase of Fe content causes lowering of the ρ .

Fig. 6 shows the core losses at 50 Hz for the melt-spun $\text{Fe}_{85}\text{Si}_2\text{B}_8\text{P}_4\text{Cu}_1$ alloy annealed at 460 °C as a function of maximum induction (B_m). The data of the nanocrystallized $\text{Fe}_{83.3}\text{Si}_4\text{B}_8\text{P}_4\text{Cu}_{0.7}$ alloy, Si-steels and the $\text{Fe}_{78}\text{Si}_9\text{B}_{13}$ typical amorphous alloy are also

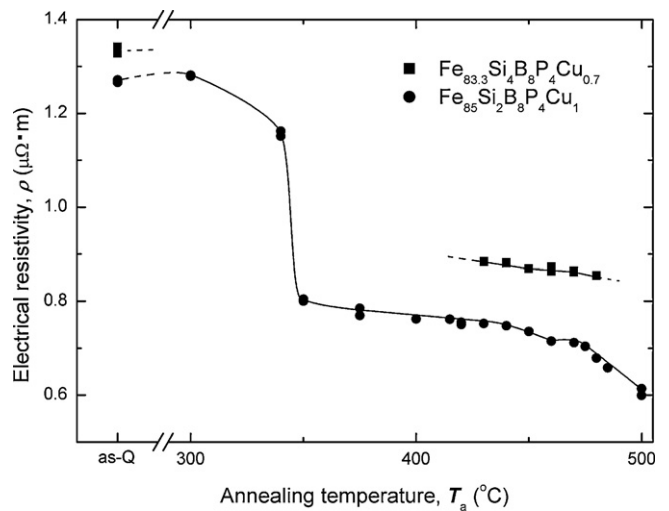


Fig. 5. Annealing temperature dependence of ρ for the melt-spun $\text{Fe}_{85}\text{Si}_2\text{B}_8\text{P}_4\text{Cu}_1$ alloy. The data of the $\text{Fe}_{85}\text{Si}_2\text{B}_8\text{P}_4\text{Cu}_1$ alloy are also shown for comparison.

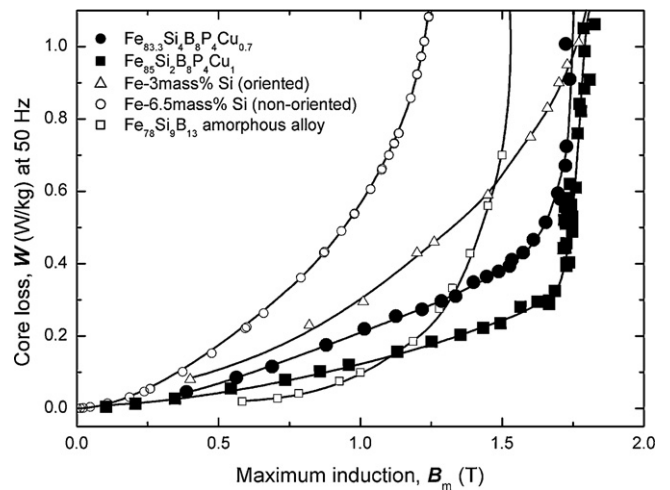


Fig. 6. Core losses (W) at 50 Hz for the nanocrystallized $\text{Fe}_{85}\text{Si}_2\text{B}_8\text{P}_4\text{Cu}_1$ alloy as a function of a maximum induction (B_m). The data of the nanocrystallized $\text{Fe}_{83.3}\text{Si}_4\text{B}_8\text{P}_4\text{Cu}_{0.7}$ alloy, Si steels and the $\text{Fe}_{78}\text{Si}_9\text{B}_{13}$ typical amorphous alloy are also shown for comparison.

shown for comparison. Both the nanocrystalline alloys sustained low W values in the B_m range of up to around 1.75 T. Comparing with the non-oriented Si-steel (Fe–6.5 mass%Si), the $\text{Fe}_{83.3}\text{Si}_4\text{B}_8\text{P}_4\text{Cu}_{0.7}$ and $\text{Fe}_{85}\text{Si}_2\text{B}_8\text{P}_4\text{Cu}_1$ alloys exhibit much small W in the while B_m range in this study. Although the $\text{Fe}_{85}\text{Si}_2\text{B}_8\text{P}_4\text{Cu}_1$ alloy showed almost same W behavior to the $\text{Fe}_{83.3}\text{Si}_4\text{B}_8\text{P}_4\text{Cu}_{0.7}$ alloy, the W of

Table 1

Average grain size (D) and magnetic and electrical properties (B_s , H_c , H_e , μ_s , λ and W) of $\text{Fe}_{83.3}\text{Si}_4\text{B}_8\text{P}_4\text{Cu}_{0.7}$, $\text{Fe}_{84.3}\text{Si}_4\text{B}_8\text{P}_3\text{Cu}_{0.7}$ and $\text{Fe}_{85}\text{Si}_2\text{B}_8\text{P}_4\text{Cu}_1$ nanocrystalline soft magnetic alloys. Data of the previously reported nanocrystalline, the representative Si steels [13] and the $\text{Fe}_{78}\text{Si}_9\text{B}_{13}$ typical amorphous alloy are also shown for comparison.

Composition (at%)	D (nm)	B_{800} (T)	B_s (T)	H_c (A/m)	μ_e (at 1 kHz)	ρ ($\mu\Omega\cdot\text{m}$)	λ_s (10^{-6})	$W_{1.5/50}$ (W/kg)	$W_{1.7/50}$ (W/kg)
$\text{Fe}_{83.3}\text{Si}_4\text{B}_8\text{P}_4\text{Cu}_{0.7}$	10	1.76	1.80	4.6	27,000	0.864	3.8	0.28	0.49
$\text{Fe}_{83.3}\text{Si}_4\text{B}_8\text{P}_3\text{Cu}_{0.7}$	17	1.80	1.84	2.6	36,000	0.812	3.1	0.27	0.47
$\text{Fe}_{85}\text{Si}_2\text{B}_8\text{P}_4\text{Cu}_1$	16	1.82	1.85	6.1	27,000	0.727	2.3	0.25	0.38
$\text{Fe}_{73.5}\text{Si}_{13.5}\text{B}_9\text{Nb}_3\text{Cu}_1$	20	1.23	1.24	0.5	150,000	1.15	2.1	–	–
$\text{Fe}_{90}\text{Zr}_7\text{B}_3$	13	1.65	1.7	5.8	29,000	0.44	–1.1	0.24	0.41
Fe–3 mass%Si									
Non-oriented type ($t=0.35$ mm)	–	1.51	2.03	26	720	0.572	6.8	2.02	3.48
Oriented, domain controlled type ($t=0.27$ mm)	–	1.92	2.03	26	720	0.572	6.8	2.02	0.84
Fe–6.5 mass%Si									
Non-oriented type ($t=0.35$ mm)	–	1.29	1.79	22	2100	0.817	0.1	2.04	–
$\text{Fe}_{78}\text{Si}_9\text{B}_{13}$ (2605)	Amo	1.49	1.54	2.6	10,600	1.35	27	0.68	–

the former alloy is superior to that of the latter alloy, and to highest-graded oriented Si-steel (Fe–3.0 mass%Si) in the B_m range of up to 1.8 T. The Fe₇₈Si₉B₁₃ amorphous alloy exhibited smallest W value among all the specimens in the B_m range of up to 1.3 T. However, the W rapidly increased by further increasing of B_m , because the B_s of the alloy is 1.56 T. On the contrary, as mentioned above, the W of the Fe–Si–B–P–Cu nanocrystalline alloys can sustain the low W up to higher B_m range of over 1.3 T due to high B_{800} and excellent magnetic softness, although those were slightly higher than that of the amorphous alloy in the B_m range of up to 1.3 T.

Table 1 summarizes the average grain size (D) of precipitated α -Fe phase and magnetic and electric properties; B_s , H_c , μ_e , λ_s , ρ and W for Fe_{83.3}Si₄B₈P₄Cu_{0.7}, Fe_{84.3}Si₄B₈P₃Cu_{0.7}, Fe₈₅Si₂B₈P₄Cu₁, the representative nanocrystalline alloys, Si-steels [10,11,13] and the Fe₇₈Si₉B₁₃ typical amorphous alloy. Here, annealing temperatures are 475 °C for Fe_{83.3}Si₄B₈P₄Cu_{0.7} and Fe_{84.3}Si₄B₈P₃Cu_{0.7}, 465 °C for Fe₈₅Si₂B₈P₄Cu₁, respectively. Although the D of the crystallized alloys mostly increased with increase in Fe content, the crystallized alloys consisted of fine α -Fe phase less than 20 nm in a diameter, which reveals the typical nanocrystalline structure [2,3,14–17]. The B_s of the Fe–Si–B–P–Cu nanocrystalline alloys is higher than 1.2–1.7 T of the conventional nanocrystalline and amorphous alloys now in practical use. In particular, the Fe₈₅Si₂B₈P₄Cu₁ nanocrystalline alloy exhibits much high B_{800} of 1.82 T comparable to the oriented Fe–3.0 mass%Si alloy and recently reported nanocrystalline alloy [18]. The H_c of these alloys are 2.6–6.1 A/m, which is superior to Si steels. The μ_e of 27,000–36,000 are higher than those of the typical amorphous alloy and Si steels. The small λ_s of $+2.3 - 3.8 \times 10^{-6}$ which are much smaller than 27×10^{-6} of the amorphous alloy, might be obtained by the nanocrystallized structures composed of α -Fe phase with negative magnetostriction and residual amorphous phase with positive magnetostriction. As a result, it is thought that above-mentioned magnetic softness is originated from the simultaneous realization of the homogeneous nanocrystalline structure and small λ_s . Therefore the Fe–Si–B–P–Cu nanocrystalline alloys exhibit very low losses ($W_{1.5/50}$ and $W_{1.7/50}$).

4. Conclusions

The Fe–Si–B–P–Cu nanocrystalline alloys exhibit significantly higher B_s and excellent magnetic softness. The conclusions obtained are summarized as follows.

1. The Fe₈₅Si₂B₈P₄Cu₁ nanocrystalline alloy exhibits extremely high B_{800} and B_s of above 1.80 T which are considerably higher than those of any soft magnetic amorphous and nanocrystalline alloys previously reported, and comparable to the highest-graded oriented Si steel now in use.
2. The Fe₈₅Si₂B₈P₄Cu₁ nanocrystalline alloy exhibits excellent magnetic softness; H_c of 6.1 A/m and μ_e of 27,000 at 1 kHz, due to the simultaneous realization of the uniform nanostructure composed by small α -Fe grains with less than 20 nm in diameters and small magnetostriction of $+2.3 \times 10^{-6}$.

The W of the Fe₈₅Si₂B₈P₄Cu₁ nanocrystalline alloy is superior to the commercial non-oriented and oriented Si-steels over the B_m range up to 1.75 T, and the alloy also exhibit higher ρ values (0.72 $\mu\Omega$ m) than the Si-steels.

References

- [1] N.P. Goss, Trans. Am. Soc. Met. 23 (1935) 511–531.
- [2] Y. Yoshizawa, S. Oguma, K. Yamauchi, J. Appl. Phys. 64 (1988) 6044–6046.
- [3] K. Suzuki, A. Makino, N. Kataoka, A. Inoue, T. Masumoto, Mater. Trans. JIM 32 (1991) 93–102.
- [4] Y. Yoshizawa, K. Yamauchi, Mater. Trans. JIM 31 (1990) 307–314.
- [5] A. Makino, T. Hatanai, Y. Naitoh, T. Bitoh, A. Inoue, T. Masumoto, IEEE Trans. Magn. 33 (1997) 3793–3798.
- [6] A. Makino, A. Inoue, T. Masumoto, Mater. Trans. JIM 36 (1995) 924–938.
- [7] H. Iwanabe, B. Liu, M.E. McHenry, D.E. Laughlin, J. Appl. Phys. 85 (1999) 4424–4426.
- [8] A. Makino, T. Bitoh, J. Appl. Phys. 93 (2003) 6522–6524.
- [9] A. Makino, H. Men, K. Yubuta, T. Kubota, J. Appl. Phys. 105 (2009), 013922 (4 pp.).
- [10] H. Men, L. Cui, T. Kubota, K. Yubuta, A. Makino, A. Inoue, Mater. Trans. 50 (2009) 1330–1333.
- [11] A. Makino, H. Men, T. Kubota, K. Yubuta, A. Inoue, Mater. Trans. 50 (2009) 204–209.
- [12] A. Makino, H. Men, T. Kubota, K. Yubuta, A. Inoue, J. Appl. Phys. 105 (2009) 07A308.
- [13] Nippon Steel Corporation, Catalog of the Non-oriented Electrical steel sheets, Available: <http://www.nsc.co.jp/en/product/sheet/pdf/EXE319.pdf>.
- [14] G. Herzer, IEEE Trans. Magn. 26 (1990) 1397–1402.
- [15] K. Suzuki, M. Kikuchi, A. Makino, A. Inoue, T. Masumoto, Mater. Trans. JIM 32 (1991) 961–968.
- [16] A. Makino, T. Bitoh, A. Inoue, T. Masumoto, Scr. Mater. 48 (2003) 869–874.
- [17] A. Makino, M. Bingo, T. Teruo, K. Yubuta, A. Inoue, J. Appl. Phys. 101 (2007), 09N117 (3 pp.).
- [18] M. Ohta, Y. Yoshizawa, Appl. Phys. Lett. 91 (2007), 062517 (3 pp.).